Polar Ordering at an Interface between a Liquid Crystal Monolayer and a Rubbed Polyimide

Masahito Oh-e, Seok-Cheol Hong, and Y. R. Shen*

Department of Physics, University of California at Berkeley, Berkeley, California 94720

Received: March 23, 2000; In Final Form: May 17, 2000

Optical second harmonic generation (SHG) was used to study how mechanical rubbing modifies the surface structure of a polyimide (poly[4,4′-oxydiphenilenepyromellitimide], PMDA-ODA) film and how the rubbed polyimide surface aligns a liquid crystal monolayer (4′-*n*-octyl-4-cyanobiphenyl, 8CB) adsorbed on it. It was found that rubbing would align the polymer chains and make the polymer surface more polar and hence more SHG active. The rubbed polymer surface would then align the adsorbed 8CB monolayer via molecule−molecule interaction in an orientational epitaxy manner. Approximate orientational distributions for molecules at the rubbed polymer surface and in the aligned 8CB monolayer were deduced from the measurements.

Introduction

Orientational ordering of liquid crystal (LC) molecules at a surface or interface is a subject not only of fundamental interest but also of technological significance. LC ordering on polymer surfaces, in particular, has attracted much attention because of its relevance to LC devices. To understand how a polymer surface orients the adsorbed LC molecules, we must first know the surface structure of the polymer. On polymers commonly used in the LC industry, such as polyimide, the LC molecules interact fairly strongly with the polymer molecular units. The surface structure of the polymer then governs the LC ordering and alignment at the surface, and hence, the surface anchoring and pretilt angle of the LC film. These are important design parameters for LC displays. So far, however, details of how a given polymer surface induces a certain LC alignment have not yet been sufficiently understood despite the fact that rubbed polyimide layers are routinely used for aligning LCs in the fabrication of LC devices. To search for a better understanding and later for a possible control of LC alignment on polymers, we need to know both the surface structure of a polymer and the orientational ordering and alignment of LC molecules adsorbed on the polymer.

In recent years, second-harmonic generation (SHG) has been developed into a viable surface analytical probe.[1,2] It is based on the principle that under the electric-dipole approximation, SHG is forbidden in media with inversion symmetry, but allowed at surfaces and interfaces where such symmetry is broken.[3] The technique has been used to study LC monolayers at surfaces and interfaces. It was found that the first LC molecular monolayer on rubbed polyimide is preferentially oriented along the rubbing direction and exhibits biaxiality.[4] On polyimide with different alkyl chain lengths, an odd−even effect of the chain length on the surface LC orientation, and hence the pretilt angle, were observed.[5] Also, from the orientational distribution of the monolayer, a quantitative description on how the LC monolayer orientation is related to the bulk pretilt angle via LC molecule−molecule correlation was established.[6−8] Shirota et al.[9−11] applied the technique to polyimide surfaces with SHG-active side chains and reported the effects of rubbing on the orientation and alignment of the side chains as well as the LC monolayer and film deposited on the polyimide.

For a better understanding on the physical mechanism of LC monolayer alignment by a polymer surface, one would like to investigate LC on a number of different polymers with known surface structures. The latter information is often difficult to obtain with SHG measurement. In most reported cases, SHG from the surface of a polymer, such as poly[*n*-alkylpyromelliticimide][4−7] and poly(vinyl alcohol),[12] is small or negligible. Only those with mesogenic side chains can yield strong surface SHG output, the measurement of which provides information on the surface orientation of the side chains.[9−11,13] We can then study how these side chains affect the orientation of the adsorbed LC monolayer and subsequently the surface anchoring and bulk pretilt angle of an LC film.

We note that other techniques have also been employed to study polyimide surfaces. Ellipsometry[14] and infrared (IR) spectroscopy[15] have been used to evaluate structural anisotropy induced by rubbing in a surface layer of several tens of nm. Atomic force microscopy[16] can reveal an image of a rubbed polymer surface, but the resolution is often not sufficient to resolve the surface molecular structure. Near-edge X-ray absorption fine structure spectroscopy[17] can probe a surface layer of 1 nm thick and has been most successful in providing surface structure of polymers. Sum-frequency vibrational spectroscopy is another viable technique for probing surface structures of materials, and has recently been applied successfully to rubbed polymer surfaces.[12]

In this paper, we report our study of surface orientational distributions of the main chain units of poly[4,4′-oxydiphenilenepyromellitimide] (PMDA-ODA) (a polyimide with no side chains) with and without rubbing and the orientational distribution of a 4′-*n*-octyl-4-cyanobiphenyl (8CB) monolayer evaporated on the polyimide surfaces using SHG. PMDA-ODA has a backbone structure similar to the polyimides used in practical LC devices. It is also one of the typical polyimides whose basic physical properties have been investigated and known. The surface layer property of PMDA-ODA has recently been studied by IR spectroscopy.[18−22] In that work, the average molecular orientation of a surface layer was deduced from the variation of IR absorption as a function of the incident angle in comparison to a theoretical model. It was found that, without rubbing, the distribution of polymer backbones was isotropic and parallel to the substrate plane and with rubbing, the

* To whom correspondence should be addressed.

10.1021/jp0011138 CCC: $19.00
Published on Web 07/18/2000

polyimide backbones preferentially oriented along the rubbing direction with an upward tilt of ~8.5°. However, as we mentioned earlier, the surface layer thickness probed in this case was not of a monolayer, but of a few nm in depth. With SHG, however, the orientation and alignment of surface monolayers are probed. We have measured SHG from PMDA-ODA surfaces, both rubbed and unrubbed, with and without an adsorbed 8CB monolayer. The quantitative results show that rubbing aligns the surface polymer chains and makes the surface more polar. Via orientational epitaxy-like interaction, the aligned surface polymer chains then effectively aligns the adsorbed 8CB monolayer.

Theoretical Background

The basic theory of SHG for surface studies has been described elsewhere.[23] Here, we briefly summarize the key points needed for analyzing our experimental results. Surface SHG originates from a nonlinear polarization induced at an interface by an incoming laser field $E(\omega)$.

$$P(2\omega) = \boldsymbol{\chi}^{(2)}:E(\omega)E(\omega) \tag{1}$$

where $\boldsymbol{\chi}^{(2)}$ denotes the surface nonlinear susceptibility tensor, characterizing the interfacial layer. The SHG output intensity in the reflected direction is given by

$$I(2\omega) \propto \sec^2 \Theta(2\omega)|\boldsymbol{\chi}^{(2)}_{\mathrm{eff}}|^2 I^2(\omega)$$

$$= \sec^2 \Theta(2\omega)|[\mathbf{e}_{2\omega}\cdot L(2\omega)]\cdot\boldsymbol{\chi}^{(2)}:[\mathbf{e}_{\omega}\cdot(\omega)] \times [\mathbf{e}_{\omega}\cdot L(\omega)]|^2 I^2(\omega) \tag{2}$$

where $\Theta(2\omega)$ is the reflection angle of incidence of the SH output, $L(\Omega)$ is the transmission Fresnel factor at frequency Ω, and e_ω is a unit vector specifying the polarization of the beam at ω. As a third-rank tensor $\boldsymbol{\chi}^{(2)}$ consists of 27 tensor elements. For molecules with a dominant hyperpolarizability element $\alpha^{(2)}_{\zeta\zeta\zeta}$ along the longitudinal molecular axis ζ, each tensor element of $\boldsymbol{\chi}^{(2)}$ can be related to $\alpha^{(2)}_{\zeta\zeta\zeta}$ as

$$\chi^{(2)}_{ijk} = N_s\langle(\hat{\imath}\cdot\hat{\zeta})(\hat{\jmath}\cdot\hat{\zeta})(\hat{k}\cdot\hat{\zeta})\rangle\alpha^{(2)}_{\zeta\zeta\zeta} \tag{3}$$

where N_s is the surface density of molecules, i, j, k refer to the lab coordinates (x, y, z) and the brackets denote an average over a molecular orientational distribution function. Surface structural symmetry makes some of the $\boldsymbol{\chi}^{(2)}$ elements vanish and some depend on others. For a unidirectionally rubbed surface with the C_{1v} symmetry, the nonvanishing elements are

$$\chi^{(2)}_{zzz} = N_s\langle\cos^3\theta\rangle\alpha^{(2)}_{\delta\delta\delta}$$

$$\chi^{(2)}_{xxx} = N_s\langle\sin^3\theta\cos^3\phi\rangle\alpha^{(2)}_{\delta\delta\delta}$$

$$\chi^{(2)}_{zyy} = \chi^{(2)}_{yzy} = \chi^{(2)}_{yyz} = N_s\langle(\cos\theta - \cos^3\theta)(1 - \cos^2\phi)\rangle\alpha^{(2)}_{\zeta\zeta\zeta}$$

$$\chi^{(2)}_{zxx} = \chi^{(2)}_{xzx} = \chi^{(2)}_{xxz} = N_s\langle(\cos\theta - \cos^3\theta)\cos^2\phi\rangle\alpha^{(2)}_{\zeta\zeta\zeta}$$

$$\chi^{(2)}_{xyy} = \chi^{(2)}_{yxy} = \chi^{(2)}_{yyx} = N_s\langle\sin^3\theta(\cos\phi - \cos^3\phi)\rangle\alpha^{(2)}_{\zeta\zeta\zeta}$$

$$\chi^{(2)}_{xzz} = \chi^{(2)}_{zxz} = \chi^{(2)}_{zzx} = N_s\langle(\sin\theta - \sin^3\theta)\cos\phi\rangle\alpha^{(2)}_{\zeta\zeta\zeta} \tag{4}$$

Here θ is the angle between $\hat{\zeta}$ and $\hat{z}$ (along the surface normal), and ϕ is the azimuthal angle between the rubbing direction x and the projection of ζ onto the $x-y$ plane. These $\boldsymbol{\chi}^{(2)}$ elements can be deduced from $|\boldsymbol{\chi}^{(2)}_{\mathrm{eff}}|$ measured by SHG with different input and output polarization combinations as functions of the azimuthal sample rotation angle ϕ between the incident plane and the anti-rubbing direction. As seen in eq 2, $\boldsymbol{\chi}^{(2)}_{\mathrm{eff}}$ is directly related to a linear combination of $\chi^{(2)}_{ijk}$. To deduce quantitative information about the molecular distribution, we assume the distribution function to have the form

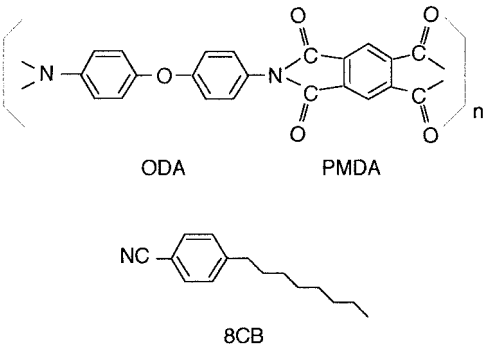

Figure 1. Chemical structures of a PMDA-ODA polyimide molecular unit and a 8CB liquid crystal molecule.

$$f(\theta,\phi) = P(\theta)Q(\phi)$$

$$P(\theta) = A\exp\left[\frac{-(\theta - \theta_0)^2}{2\sigma^2}\right]$$

$$Q(\phi) = 1 + d_1\cos\phi + d_2\cos 2\phi + d_3\cos 3\phi \tag{5}$$

With this explicit form of $f(\theta,\phi)$, eq 3 allows us to determine all the unknown parameters, θ_0, σ, d_1, d_2, and d_3, in $f(\theta,\phi)$ from the measured values of $\chi^{(2)}_{ijk}$, thus providing a quantitative description of the orientational distribution of the surface molecules.

Experimental Section

Figure 1 illustrates the chemical structures of PMDA-ODA and 8CB. In our experiments, the polyimide samples with a layer thickness of ~20 nm were prepared by spin coating. To obtain uniform layers, the PMDA-ODA polyamic acid solution was filtered with membrane filters. It was then dropped on a substrate to be spin-coated at 3500 rpm for 60 s. For the imidization reaction, the samples were baked at 250 °C for 20 min. Rubbing to align the polyimide surface structure to the saturation level was carried out by a rubbing machine with a velvet cloth. Monolayers of 8CB were deposited on the polyimide-coated substrates by evaporation at 70 °C and monitoring SHG signals in situ. The SHG output from the surface appeared saturated when the 8CB deposition reached a monolayer.

The experimental setup for the surface SHG measurement has been described elsewhere.[1,2,23] Briefly, the input beam was from a frequency-doubled Q-switched mode locked YAG laser and the SHG output in reflection from the sample surface was recorded. The angle of incidence was set at 67°. The SHG was measured as a function of the sample azimuthal angle for four different input and output polarization combinations, i.e., s-in/p-out, p-in/p-out, p-in/s-out, and s-in/s-out.

To separate $\boldsymbol{\chi}^{(2)}$ for the 8CB monolayer from $\boldsymbol{\chi}^{(2)}_{\mathrm{total}}$ for 8CB on polyimide, we need to know the phase of $\boldsymbol{\chi}^{(2)}_{\mathrm{eff}}$. This can be measured by the usual SHG interference method. In our experiments, the SHG output from the sample was set to interfere with SHG from a z-cut quartz plate in the same optical beam path and a rotatable fused silica plate was inserted between

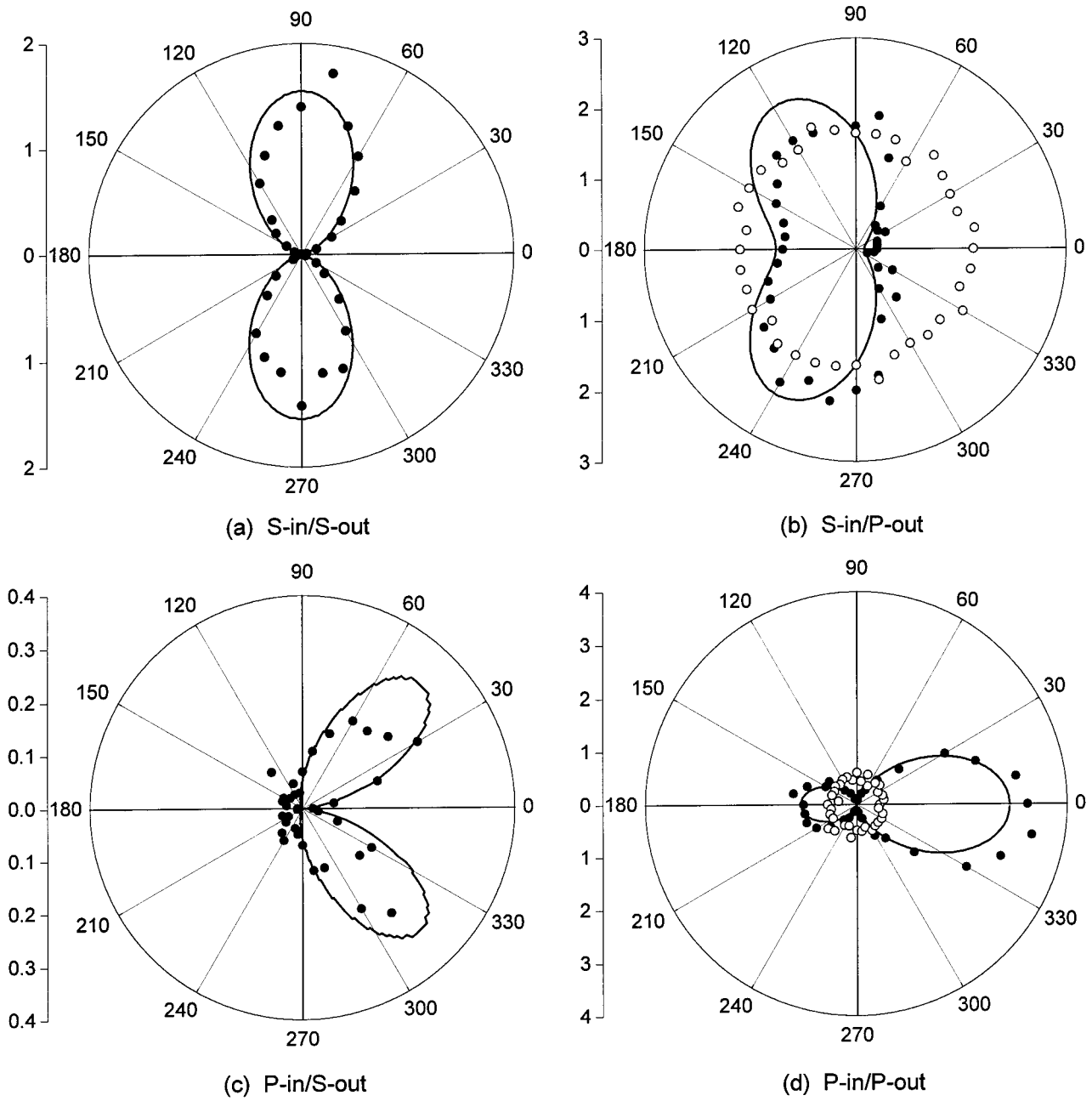

Figure 2. Polar plots of SHG from rubbed (solid circles) and unrubbed (open circles) PMDA-ODA surfaces. Solid lines are the theoretical fit. (a), (b), (c). and (d) are for s-in/s-out, s-in/p-out, p-in/s-out, and p-in/p-out polarization combinations, respectively.

the two to vary their relative phase and generate the SHG interference pattern.[24−28] Comparing the interference patterns from polyimide samples with and without the 8CB monolayer, we could deduce the relative phases of $\chi^{(2)}_{\text{eff}}$.

Results

We first measured SHG from the PMDA-ODA surfaces, both rubbed and unrubbed. For the rubbed surface, the SHG signal as a function of azimuthal angle Φ of the sample orientation is shown in Figure 2, where Φ is defined as the angle between the plane of incidence and the antirubbing direction. For all input/output polarization combinations, the data appear to be anisotropic with a symmetric axis along the rubbing direction (from 0° to 180°). There is also a clear forward/backward asymmetry in the rubbing direction. For the unrubbed surface, the signal is negligibly small and isotropic in Φ. This indicates that rubbing had significantly altered the surface structure of PMDA-ODA. First, the surface polymer chains must have more or less been aligned by rubbing along the rubbing direction, and second, rubbing must have also induced tilts of molecular units in the surface polymer chains and the tilts are not the same in the forward and backward direction. We also found in the unrubbed case, $\chi^{(2)}_{yzy} \cong \chi^{(2)}_{cyy}$ within 20%. According to eq 4, this suggests that we can crudely approximate the polymer molecular units as an effective rodlike molecule with a dominantly polarizability element $\alpha^{(2)}_{\zeta\zeta\zeta}$. In any case, we can use eq 2 to fit the experimental data in Figure 2 and deduce the nonvanishing $\chi^{(2)}_{ijk}$ for the rubbed PMDA-ODA surface. The Fresnel coefficients $L(\omega)$ were calculated using refractive index values $n_{q1} = 1.46$ and $n_{p1} = 1.7$ for quartz and polyimide,[20] respectively, at 532 nm and $n_{q2} = 1.50$ and $n_{p2} = 1.96 + i0.43$ at 266 nm. The imaginary part of n_{p2} was determined by absorption measurement. The real part of n_{p2} was optimized in the fitting procedure for finding $\chi^{(2)}_{ijk}$. We also assumed $n = 1$ for the

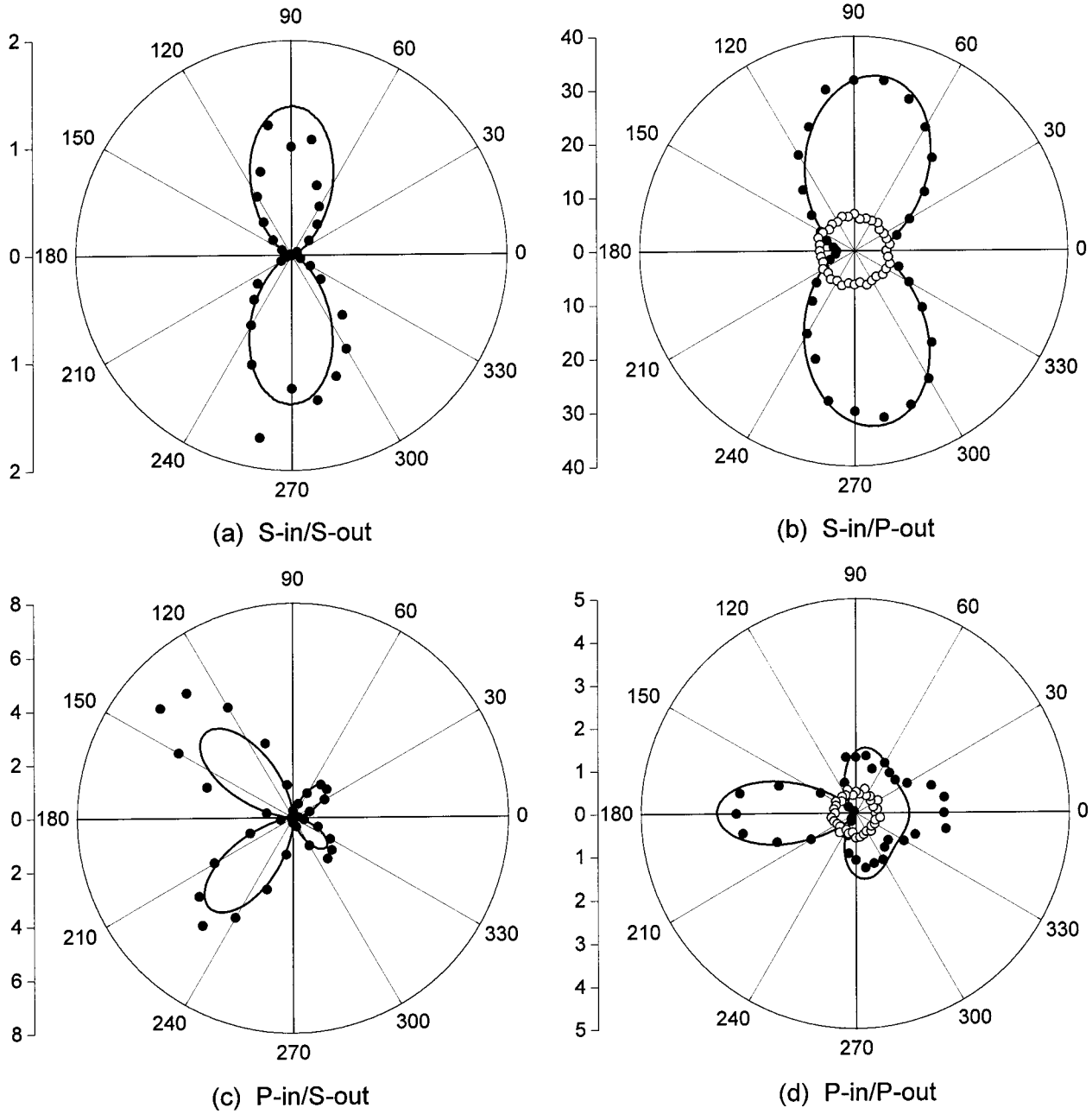

Figure 3. Polar plots of SHG from rubbed (solid circles) and unrubbed (open circles) PMDA-ODA surface with an 8CB monolayer on it. Solid lines are the theoretical fit. (a), (b), (c), and (d) are for s-in/s-out, s-in/p-out, p-in/s-out, and p-in/p-out polarization combinations, respectively.

surface of PMDA-ODA. As seen in Figure 2, the fit is good, from which we find (with $\chi^{(2)}_{ijk}$ normalized to $\chi^{(2)}_{xxx}$.) $\chi^{(2)}_{xxx}$:$\chi^{(2)}_{xyy}$:$\chi^{(2)}_{xzz}$:$\chi^{(2)}_{zxx}$:$\chi^{(2)}_{zyy}$:$\chi^{(2)}_{zzz}$ = −1.00:−0.22:−0.0029:0.34:0.18:0.023.

We next measured SHG from an 8CB monolayer on the rubbed and unrubbed PMDA-ODA surfaces. Figure 3 shows the plot of SHG as a function of Φ for four different polarization combinations. The data for the unrubbed case are also presented in Figure 3. As expected for an isotropic monolayer, SHG from 8CB on unrubbed PMDA-ODA was isotropic with nonvanishing signals in the p-in/p-out and s-in/p-out polarization combinations. The results yield the ratio $\chi^{(2)}_{zyy}/\chi^{(2)}_{zzz} = 3.2$ for the isotropic 8CB monolayer.

On rubbed PMDA-ODA with an adsorbed 8CB monolayer, the SHG signal shows an anisotropy with mirror symmetry about the rubbing direction. As seen in Figure 3, SHG from the 8CB monolayer clearly dominants in the p-in/s-out and s-in/p-out polarization combinations. For s-in/s-out and p-in/p-out, the signal from PMDA-ODA is significant. In the latter cases, we found that as the surface density of 8CB increased from zero, the SHG signal first decreased and then increased, reaching a saturation value at the full monolayer. The nonlinear susceptibility of the 8CB monolayer apparently has a phase nearly opposite to that of PMDA-ODA.[28] The p-in/p-out result shows that the signal is stronger along, than opposite to, the rubbing direction. It indicates that the 8CB molecules are aligned preferentially along the rubbing direction. The s-in/s-out result shows $|\chi^{(2)}_{8CB+PI}|_{SS} \cong |\chi^{(2)}_{PI}|_{SS}$ and since $\chi^{(2)}_{8CB}$ and $\chi^{(2)}_{PI}$ are nearly out of phase, we have $|\chi^{(2)}_{8CB}| \approx 2|\chi^{(2)}_{PI}|$. For all polarization combinations, SHG from an 8CB monolayer as a function of Φ appears to be symmetric about the rubbing axis. Again, using eq 2, we could obtain a fit of the data for 8CB on PMDA-ODA as shown in Figure 3. From the fit, we deduced the ratios of the nonvanishing $\chi^{(2)}$ elements for 8CB on PMDA-ODA. They are: $\chi^{(2)}_{xxx}$:$\chi^{(2)}_{xyy}$:$\chi^{(2)}_{xzz}$:$\chi^{(2)}_{zxx}$:$\chi^{(2)}_{zyy}$:$\chi^{(2)}_{zzz}$ = 1.00:0.14:0.018:1.87:0.70:0.39.

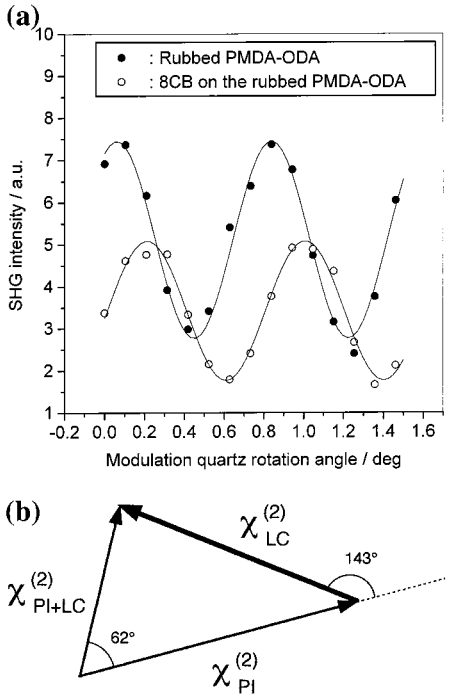

Figure 4. (a) SHG interference patterns from a rubbed PMDA-ODA surface with and without an 8CB monolayer. The measurement was performed with a p-in/p-out polarization combination and the sample azimuthal angle at 0°. (b) Schematic illustration of the relative amplitude and phase relation among $\vec{\chi}^{(2)}_{PI}$, $\vec{\chi}^{(2)}_{PI+LC}$, and $\vec{\chi}^{(2)}_{LC}$.

For 8CB on PMDA-ODA, we have $\vec{\chi}^{(2)}_{8CB+PI} \cong \vec{\chi}^{(2)}_{8CB} + \vec{\chi}^{(2)}_{PI}$. To find $\vec{\chi}^{(2)}_{8CB}$ for the 8CB monolayer, we need to subtract $\vec{\chi}^{(2)}_{PI}$ from $\vec{\chi}^{(2)}_{8CB+PI}$. However, because $\vec{\chi}$s are complex in general, we must also know the relative phase between $\vec{\chi}^{(2)}_{8CB+PI}$ and $\vec{\chi}^{(2)}_{PI}$. This was achieved by the phase measurement described earlier. Figure 4 indicates a phase shift of 62° for $\vec{\chi}^{(2)}_{8CB+PI}$ relative to $\vec{\chi}^{(2)}_{PI}$, and accordingly, $\vec{\chi}^{(2)}_{8CB}$ leads $\vec{\chi}^{(2)}_{PI}$ by 143°. This is consistent with the earlier conclusion that $\vec{\chi}^{(2)}_{8CB}$ and $\vec{\chi}^{(2)}_{PI}$ appear to be out of phase.

Knowing the phase difference between $\vec{\chi}^{(2)}_{8CB+PI}$ and $\vec{\chi}^{(2)}_{PI}$, we can now find from

$$|\chi^{(2)}_{LC}| = -|\chi^{(2)}_{PI}| \cos 143° + \sqrt{|\chi^{(2)}_{PI+LC}|^2 - |\chi^{(2)}_{PI}|^2 \sin^2 143°} \quad (6)$$

the values of $\vec{\chi}^{(2)}_{8CB}$ as a function of Φ for all the polarization combinations. Figure 5 shows the polar plot of the deduced $\vec{\chi}^{(2)}_{8CB}$ versus Φ. From the theoretical fit, we find for the 8CB monolayer, $\chi^{(2)}_{xxx}:\chi^{(2)}_{xyy}:\chi^{(2)}_{xzz}:\chi^{(2)}_{zxx}:\chi^{(2)}_{zyy}:\chi^{(2)}_{zzz} = 1.00:0.15:0.0072:0.97:0.37:0.15$.

Discussion

We can use eq 4 and the measured values of $(\chi^{(2)}_{8CB})^{ijk}$ to deduce quantitative information about the molecular orientation and alignment of the 8CB monolayer on PMDA-ODA. On the unrubbed polymer surface, we have, from eq 4 with $\langle\cos^2\Phi\rangle = 1/2$ for an isotropic azimuthal distribution, $\chi^{(2)}_{zyy}/\chi^{(2)}_{zzz} = \langle\sin^2\theta\cos\theta\rangle/2\langle\cos^3\theta\rangle = 3.2$. If we assume a δ-function for the molecular orientational distribution in θ, then we find that the 8CB molecules are tilted by $\theta = 68°$ away from the surface normal.

On the rubbed PMDA-ODA surface, Figure 5 shows explicitly that the 8CB molecules are preferentially aligned along the rubbing axis. The forward/backward asymmetry has been interpreted as a better alignment of the 8CB molecules along the rubbing direction.[4] The result is consistent with the positive bulk pretilt angle of 8CB alignment along the rubbing direction in a film sandwiched between two rubbed PMDA-ODA-coated substrates. It is also similar to those reported on nCB on poly-[*n*-alkylpyromellitimide] and poly(vinyl alcohol) coated substrates. To obtain quantitative information about the orientation and alignment of 8CB on rubbed PMDA-ODA from the measured $(\chi^{(2)}_{8CB})_{ijk}$, we use the orientational distribution function of eq 5. Then with eq 4, we find $\theta_0 = 79.7°$, $\sigma = 9.5$, $d_1 = 0.34$, $d_2 = 0.90$, and $d_3 = 0.18$. We note that the rubbing-induced surface structure of PMDA-ODA does affect the azimuthal distribution of 8CB molecules.

The data in Figures 2 and 3 for rubbed PMDA-ODA without 8CB also exhibit an anisotropy with mirror symmetry about the rubbing axis. There also exists a forward/backward asymmetry, but surprisingly, it is opposite to the alignment of the 8CB monolayer adsorbed on the surface. To understand this result, we refer to the repeated molecular units of PMDA-ODA shown in Figure 6. The PMDA-ODA film is known to have a crystalline like structure, but macroscopically it is amorphous. X-ray diffraction reveals a unit cell (Figure 6) which is orthorhombic with lattice parameters of 6.31, 3.97, and 32 Å along the *a*, *b*, and *c* axes, respectively.[29] Each unit cell is composed of two PMDA-ODA sections in a zigzag configuration. At the surface, if the $a-c$ plane is nearly parallel to the surface, then because each PMDA-ODA section has an inversion symmetry, little SHG is expected from the surface. Presumably this is the case with the unrubbed PMDA-ODA surface, which also has an isotropic azimuthal distribution of molecular orientation. Rubbing pulls the surface polymer chains, causing them to more or less align in the rubbing direction. The increased SHG signal indicates that the *b*-axis of the molecular units (Figure 6) at the surface must have tilted away from the surface so that the inversion symmetry of each PMDA-ODA section is broken by the different environments its two ends experience. We can use a vector along the long axis of each PMDA-ODA section to denote polar ordering of the surface structure. The stronger SHG signal in the anti-rubbing direction means that the backward pointing vectors have a smaller tilt angle (from the surface normal) than the forward pointing ones, or the rubbing-aligned *c*-axis at the surface has a small upward tilt. Alternately, it has been proposed that rubbing causes the molecular arrangement in the unit cell (Figure 6) to deform into an asymmetric triangular configuration with the backward tilting section having a smaller tilt. The latter model was used to explain the observed tilt of the principal axis of the linear dielectric constant from the surface induced by rubbing.[20]

With the above picture for the PMDA-ODA surface, it is no longer appropriate to use $f(\theta,\phi)$ in eq 5 as the orientational distribution for the PMDA-ODA sections, since the distributions in polar and azimuthal coordinates should be coupled. In this case, we can assume $f(\theta,\phi)$ to have the form $f(\theta,\phi) = A'\exp[-(\theta - \theta_0 + a_1\cos\phi + a_2\cos 2\phi)^2/\sigma^2](1 + d\cos 2\phi)$ with θ_0, σ, a_1, a_2, and d as coefficients. This is a simple distribution function that still has five adjustable parameters, but has θ and ϕ coordinates coupled. Treating PMDA-ODA section as a rodlike polar molecule and using the above $f(\theta,\phi)$ and the measured $(\chi^{(2)}_{PI})_{ijk}$ in eq 4, we find $\theta_0 = 83°$, $\sigma = 4.5°$, $a_1 =$

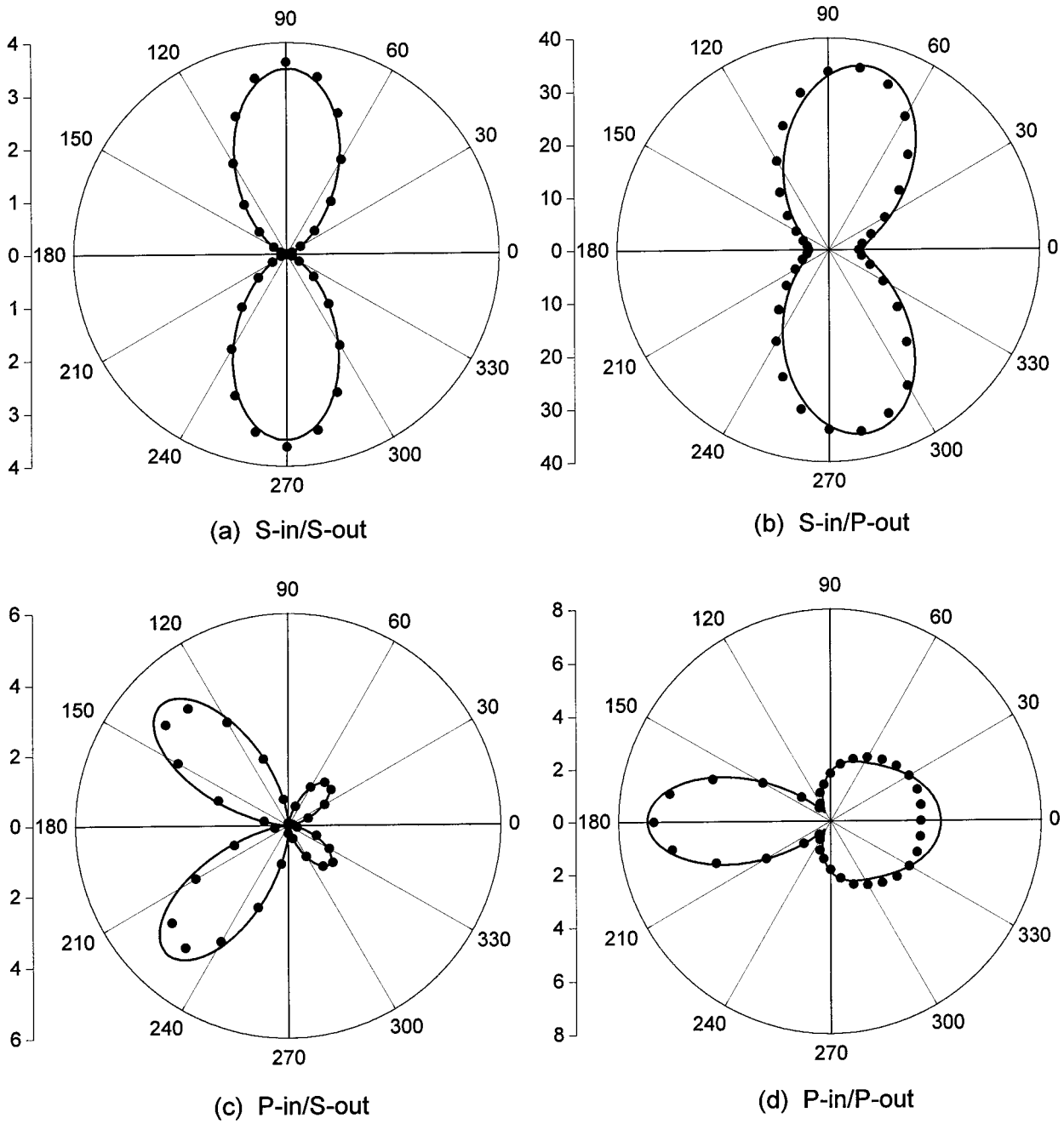

Figure 5. Polar plots of SHG from an 8CB monolayer that was adsorbed on rubbed PMDA-ODA. Data points were deduced from results in Figures 2 and 3.

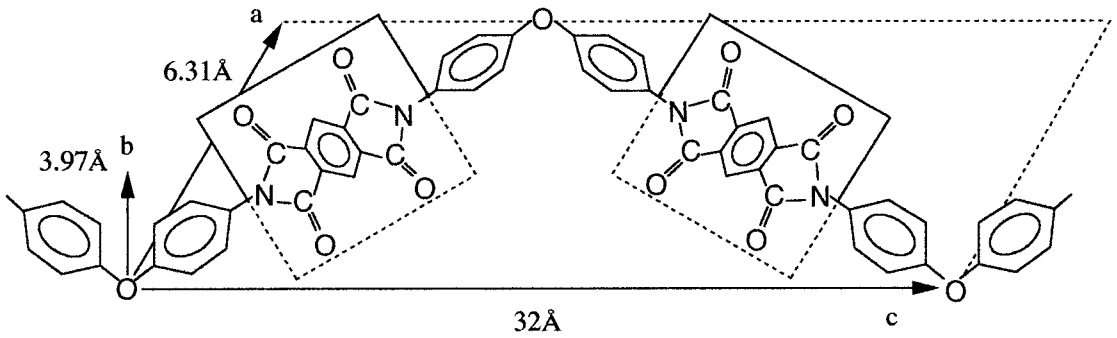

Figure 6. Local unit structure of PMDA-ODA (see refs 20 and 29).

-0.11, $a_2 = 0.01$, and $d = 0.58$. The negative sign of a_1 describes explicitly the smaller molecular tilt in the backward direction displayed by the forward/backward asymmetry.

The alignment of the 8CB monolayer on a rubbed PMDA-ODA surface is obviously due to interaction between 8CB molecules and the aligned polymer chains. The nearly opposite

phases of $\vec{\chi}_{8CB}^{(2)}$ and $\vec{\chi}_{PI}^{(2)}$ indicate that the polarity of the surface PMDA-ODA sections is opposite to that of the adsorbed 8CB molecules. The opposite forward/backward asymmetries of $\vec{\chi}_{8CB}^{(2)}$ and $\vec{\chi}_{PI}^{(2)}$ can be explained by the larger overall surface area of the forward-tilting PMDA-ODA sections available for 8CB adsorption.

From the orientational distributions deduced from the SHG measurements, we can calculate the orientational order parameters for the PMDA-ODA surface and the 8CB monolayer. The tensorial order parameter is defined in the usual way.[30,31]

$$Q_{ij} = \frac{1}{N}\sum_{k=1}^{N}\frac{(3l_i^k l_j^k - \delta_{ij})}{2} = \left\langle \frac{3}{2}(l_i l_j - \delta_{ij}) \right\rangle \tag{7}$$

where l_i and l_j are components of a unit vector along the longitudinal axis of molecule and δ_{ij} is the unit matrix. In the lab coordinates (x, y, z), with x along the rubbing direction and z along the surface normal, Q_{ij} is not diagonalized, but takes the form

$$Q_{ij} = \begin{pmatrix} \left(1 - \frac{3}{2}\sin^2\theta_s\right)S - \left(\frac{1}{2}\sin^2\theta_s\right)P & 0 & \frac{1}{4}\sin 2\theta_s(3S+P) \\ 0 & -\frac{1}{2}(S-P) & 0 \\ \frac{1}{4}\sin 2\theta_s(3S+P) & 0 & \left(1 - \frac{3}{2}\cos^2\theta_s\right)S - \left(\frac{1}{2}\cos^2\theta_s\right)P \end{pmatrix} \tag{8}$$

where θ_s is the angle between the director (in the $x-z$ plane) and the x-axis, S is the uniaxial scalar order parameter, and P denotes the biaxiality. In terms of the distribution function of eq 5, we have[6,7]

$$S = \frac{3}{4}\langle\sin^2\theta\rangle - \frac{1}{2} + \frac{3}{8}\langle\sin^2\theta\rangle d_2 \tag{9}$$

$$P = \frac{9}{4}\langle\sin^2\theta\rangle - \frac{3}{2} - \frac{3}{8}\langle\sin^2\theta\rangle d_2 \tag{10}$$

We then find for the rubbed PMDA-ODA surface, $S = 0.44$ and $P = 0.48$, and for the 8CB monolayer on the rubbed PMDA-ODA, $S = 0.52$ and $P = 0.29$. We notice that the S parameters for the two cases are not the same but very close, suggesting that the 8CB monolayer follows closely the alignment of the rubbed polymer surface. The biaxiality, however, is not necessarily transferable.

Conclusion

We have used SHG to study PMDA-ODA surfaces, rubbed and unrubbed, with and without an adsorbed 8CB monolayer. It was found that rubbing not only induces a surface mirror symmetry but also significantly increases the surface SHG signal. Clearly, rubbing must have aligned the surface PMDA-ODA chains in such a way that the molecular units appear polar at the air/polymer interface although they should be nonpolar in the bulk polymer. We believe that the zigzag molecular units in the surface PMDA-ODA chains now protrude out of the surface plane. They are also tilted in the rubbing direction to yield a stronger SHG in the antirubbing direction. The 8CB monolayer adsorbed on the rubbed PMDA-ODA surface is aligned by interaction with the polymer chains. The forward/backward asymmetry indicates that there are more 8CB molecules aligned along the rubbing direction. Quantitative analysis of the experimental data allows the deduction of orientational distributions for molecular units at the surface of rubbed PMDA-ODA and molecules in the 8CB monolayer. From the distributions, the uniaxial order parameters for the PMDA-ODA surface and the 8CB monolayer can be calculated. That the two are nearly equal is a manifestation of the epitaxial-like alignment of a liquid crystal monolayer by a rubbed polymer surface.

Acknowledgment. This work was supported by U.S. National Science Foundation Grant DMR-9704384 and Hitachi, Ltd. in Japan. We thank Dr. Takao Miwa of Hitachi Research Laboratory for providing us the polyimide used in this study.

References and Notes

(1) Shen, Y. R. *Annu. Rev. Phys. Chem.* **1989**, *40*, 327.
(2) Shen, Y. R. *Nature* **1990**, *337*, 4480.
(3) Shen, Y. R. *The Principles of Nonlinear Optics*; Wiley: New York, 1984.
(4) Chen, W.; Feller, M. B.; Shen, Y. R. *Phys. Rev. Lett.* **1989**, *63*, 2665.
(5) Johannsmann, D.; Zhou, H.; Sonderkaer, P.; Wierenga, H.; Myrvold, B. O.; Shen, Y. R. *Phys. Rev.* **1993**, E 48, 1889.
(6) Zhuang, X.; Marrucci, L.; Shen, Y. R. *Phys. Rev. Lett.* **1994**, *73*, 1513.
(7) Zhuang, X.; Marrucci, L.; Johannsmann, D.; Shen, Y. R. *Mol. Cryst. Liq. Cryst.* **1995**, *262*, 35.
(8) Barmentlo, M.; Hollering, R. W. J.; van Aerle, N. A. J. M. *Phys. Rev.* **1992**. *A46*, R4490.
(9) Shirota, K.; Ishikawa, K.; Takezoe, H.; Fukuda, A.; Shiibashi, T. *Jpn. J. Appl. Phys.* **1995**, *34*, L316.
(10) Shirota, K.; Yaginuma, M.; Ishikawa, K.; Takezoe, H.; Fukuda, A. *Nonlin. Opt.* **1996**, *15*, 93.
(11) Shirota, K.; Yaginuma, M.; Sakai, T.; Ishikawa, K.; Takezoe, H.; Fukuda, A. *Appl. Phys. Lett.* **1996**, 69, 164.
(12) Wei, X.; Zhuang, X.; Hong, S.-C.; Goto, T.; Shen, Y. R. *Phys. Rev. Lett.* **1999**, *82*, 4256.
(13) Sakai, T.; Yoo, J. G.; Kinoshita, Y.; Ishikawa, K.; Takezoe, H.; Fukuda, A.; Nihira, T.; Endo, H. *Appl. Phys. Lett.* **1997**, *71*, 2274.
(14) Hirosawa, I. *Jpn. J. Appl. Phys.* **1996**, *35*, 5873.
(15) Hasegawa, R.; Mori, Y.; Sasaki, H.; M. Ishibashi, M. *Jpn. J. Appl. Phys.* **1996**, 35, 3492.
(16) Zhu, Y. M.; Wang, L.; Lu, Z. H.; Wei, Y.; Chen, X. X.; Tang, J. H. *Appl. Phys. Lett.* **1994**, *65*, 49.
(17) Ouchi, Y.; Mori, I.; Sei, M.; Ito, E.; Araki, T.; Ishii, H.; Seki, K.; Kondo, K. *Physica B* **1995**, *208*/*209*, 407.
(18) Sakamoto, K.; Arafune, R.; Ito, N.; Ushioda, S. *Jpn. J. Appl. Phys.* **1994**, *33*, L1323.
(19) Arafune, R.; Sakamoto, K.; Yamakawa, D.; Ushioda, S. *Surf. Sci.* **1996**, *368*, 208.
(20) Sakamoto, K.; Arafune, R.; Ito, N.; Ushioda, S. *J. Appl. Phys.* **1996**, *80*, 431.
(21) Sakamoto, K.; Abe, N.; Arafune, R.; Ushioda, S. *Mol. Cryst. Liq. Cryst.* **1997**, 299, 169.
(22) Arafune, R.; Sakamoto, K.; Ushioda, S. *Appl. Phys. Lett.* **1997**, *71*, 2755.
(23) Feller, M. B.; Chen, W.; Shen, Y. R. *Phys. Rev.* **1991**, A 43, 6778.
(24) Huang, J. Y.; Lewis, A. *Biophys. J.* **1989**, *55*, 835.
(25) Berkovic, G.; Shvartsberg, E. *Appl. Phys.* **1991**, B 53, 333.
(26) Schwarzberg, E.; Berkovic, G.; Marowsky, G. *Appl. Phys.* **1994**, *A59*, 631.
(27) Kajikawa, K.; Wang, L.-M.; Isoshima, T.; Wada, T.; Knoll, W.; Sasabe, H.; Okada, S.; Nakanishi, H. *Thin Solid Film* **1996**, 284−285, 612.
(28) Sakai, T.; Shirota, K.; Yamada, T.; Hoshi, H.; Ishikawa, K.; Takezoe, H.; Fukuda, A. *Jpn. J. Appl. Phys.* **1996**, *35*, 3971.
(29) Kazaryan, L. G.; Tsvankin, D. Ya.; Ginsburg, B. M.; Tuichiev, Sh.; Korzhavin, L. N.; Frenkel, S. Ya. *Vysokomol. Soed.* **1972**, A 14, 1199. (*Polym. Sci. USSR* **1972**, *14*, 1344.)
(30) Priestley, E. B.; Wojtowicz, P. J.; Sheng, P. *Introduction to Liquid Crystals*; Plenum: New York, 1974.
(31) de Gennes, P. G.; Prost, J. *The Physics of Liquid Crystals*, 2nd ed.; Claredon: Oxford, 1993.